International Journal of Pharmaceutics 362 (2008) 60–66

Contents lists available at ScienceDirect

International Journal of Pharmaceutics

journal homepage: www.elsevier.com/locate/ijpharm

Lipid composition and grafted PEG affect in vivo activity of liposomal mitoxantrone

ChunLei Li[a,*], JingXia Cui[b], CaiXia Wang[a], JinXu Wang[a], YanHui Li[a], Lan Zhang[a], Li Zhang[a], WenMin Guo[a], YongLi Wang[b]

[a] ZhongQi Pharmaceutical Technology (Shijiazhuang) Co., Ltd., No. 276, ZhongShan West Road, Shijiazhuang City, Hebei Province 050051, PR China
[b] School of Pharmacy, Hebei Medical University, No. 361, ZhongShan East Road, Shijiazhuang City, Hebei Province 050017, PR China

ARTICLE INFO

Article history:
Received 3 May 2008
Received in revised form 4 June 2008
Accepted 10 June 2008
Available online 13 June 2008

Keywords:
Mitoxantrone
Liposomes
Lipid composition
Drug release
Antitumor efficacy
Toxicity
Polyethylene glycol grafting density

ABSTRACT

Mitoxantrone was encapsulated into pegylated SUVs using ammonium sulfate gradient method. Four formulations (LM-s, LM-p, LM-m and LM-m-L) were prepared, which were made from different PCs and exhibited different PEG grafting density. In vitro release studies revealed that drug release rate increased with decreased T_m of PCs, and reduced PEG polymer coverage. In circulation, the trend towards increased circulation time as T_m of PCs and PEG lipid content are elevated is observed. However, it was found that the order of toxicity in balb/c mice was Lm-s < LM-p < LM-m-L < LM-m. Biodistribution studies revealed that the accumulation of LM-s into tumor was ~12 times as large as that of free MIT. In s-180 tumor model, LM-s exhibited significant antineoplastic effects. Following the injection of LM-s (4 mg/kg), tumor growth was considerably inhibited, resulting in a tumor inhibition ratio of ~92%. In contrast, the treatment with free MIT exhibited almost no antitumor efficacy. In conclusion, PC composition and PEG grafting density could exert influences on the biological activity of liposomal MIT; and encapsulation of MIT into HSPC/chol SUVs with high PEG grafting density could considerably improve the therapeutic index of MIT.

1. Introduction

Mitoxantrone is a synthetic anthracenedione that has been approved for the treatment of multiple sclerosis (Martinelli Boneschi et al., 2005; Fox, 2006; Neuhaus et al., 2006), prostate cancer (Mike et al., 2006) and acute nonlymphocytic leukemia (Tallman et al., 2005). The main mechanism of action of MIT lies in that it could intercalate into DNA through hydrogen bonding, and cause crosslinks and strand breaks (Koeller and Eble, 1988). MIT also interferes with RNA and is a potent inhibitor of topoisomerase ii, an enzyme responsible for uncoiling and repairing damaged DNA (Wiseman and Spencer, 1997).

The use of MIT has been associated with cardiotoxicity, bone marrow suppression and primarily neutropenia (Cohen and Mikol, 2004). Furthermore, secondary acute myelogenous leukemia has been also reported in patients treated with MIT (Murray, 2006).

Liposomal encapsulation might alter plasma pharmacokinetics and biodistribution of chemotherapeutic agents, and selectively deliver drugs into malignant zones, thus resulting in reduced toxicity and enhanced effects (Samad et al., 2007). To realize "passive targeting" effects, the size of liposomes should be well controlled and not exceed 150 nm so that vesicles could effectively extravasate the leaky blood vessels in tumor (Drummond et al., 1999). Usually, small unilamellar vesicles (SUVs) and large unilamellar vesicles (LUVs) are employed in the development of antineoplastic liposomal formulations intended for intravenous administration.

The representative examples are two marketed liposomal products-Doxil and DaunoXome (Drummond et al., 1999). Doxil is a pegylated LUV formulation encapsulating doxorubicin. In contrast, daunoxome is a SUV formulation containing daunorubicin.

MIT has been encapsulated into liposomes via at least two kinds of methods, including intercalation into lipid bilayer via the formation of complexes with negatively charged lipids (Ahmad et al., 2005; Schwendener et al., 1991; Pestalozzi et al., 1992, 1995; Genne et al., 1994; Gokhale et al., 2001; Johnson et al., 2004; Ugwu et al., 2005), and entrapment within internal water pool using pH gradient methods (Chang et al., 1997; Adlakha-Hutcheon et al., 1999; Madden et al., 1990; Lim et al., 1997, 2000a,b). It has been reported that when MIT was loaded into LUVs made from DSPC/chol with pH gradient method, it was hard to release from vesicles, and exhibited inferior efficacy relative to free MIT (Chang et al., 1997; Adlakha-Hutcheon et al., 1999; Madden et al., 1990; Lim et al., 1997, 2000a,b).

We have previously proved that the reduction of vesicle size could accelerate the release rate of doxorubicin from pegylated

* Corresponding author. Tel.: +86 311 87891958; fax: +86 311 87885233.
E-mail addresses: lcllib@hotmail.com, lcllib@yahoo.com (C. Li).

0378-5173/$ – see front matter © 2008 Elsevier B.V. All rights reserved.
doi:10.1016/j.ijpharm.2008.06.008

Table 1
The formulation information of liposomal mitoxantrones

Formulations	Lipid composition (PC/chol, mol/mol)	PEG-lipid grafting density (% mol relative to PC)	Vesicle size (zeta average)	Polydispersion index	Entrapment efficiency (%)	T_m of PC
LM-s	HSPC/chol, 3:2	8.0	65.6	0.252	96.9	52
LM-p	DPPC/chol, 3:2	8.0	62.5	0.212	98.1	41
LM-m	DMPC/chol, 3:2	8.0	64.4	0.261	99.2	21
LM-m-L	DMPC/chol, 3:2	0.8	66.7	0.229	98.7	21

PC: phosphatidylcholine; chol: cholesterol; HSPC: hydrogenated soy PC; DPPC: 1,2-dipalmitoyl-*sn*-glycero-3-phosphocholine; DMPC: 1,2-dimyristoyl-*sn*-glycero-3-phosphocholine; PEG-lipid: 1,2-distearoyl-*sn*-glycero-3-phosphoethanolamine-*N*-[methoxy(polyethylene glycol)-2000]; T_m: transition temperature of PC from gel to liquid crystalline status.

HSPC/chol vesicles (Cui et al., 2007), thus the encapsulation of MIT into pegylated SUVs might improve its release kinetics. To obtain the optimum formulations, four kinds of vesicles were prepared, which had different lipid composition and PEG polymer coverage. The effects of these two factors on the biological activity of liposomal MIT formulations are investigated systemically. It was found that encapsulation of MIT into HSPC/chol SUVS with high PEG grafting density could considerably improve the therapeutic index of MIT.

2. Materials and methods

2.1. Materials

Mitoxantrone hydrochloride was provided by Chongqing Kailin Pharmaceutical Co., Ltd. (Chongqing, China). 1,2-Dimyristoyl-*sn*-glycero-3-phosphocholine (DMPC), 1,2-dipalmitoyl-*sn*-glycero-3-phosphocholine (DPPC) and hydrogenated soybean phosphatidylcholine (HSPC) were kind gifts from Degussa (Freising, Germany).

N-(Carbonyl-methoxypolyethyleneglycol$_{2000}$)-1,2-distearoyl-*sn*-glycero-3-phosphoethanolamine, sodium salt (MPEG$_{2000}$-DSPE) was purchased from Genzyme Pharmaceuticals (Liestal, Switzerland). Cholesterol (Chol) and Sephadex G-75 (medium) were obtained from the Sigma Chemical Company (St. Louis, MO). All other chemicals used in this study were analytical or high-performance liquid chromatography (HPLC) grade.

2.2. Preparation of liposomes

Liposomes were prepared according to following procedure. Briefly, the mixture of PC, mPEG$_{2000}$-DSPE and Chol were solubilized in chloroform and dried to a thin lipid film under a stream of N_2 gas, followed by incubation overnight under vacuum to remove residual solvent. The dried lipid films were subsequently hydrated with 300 mM ammonium sulfate. The hydration process was performed at 60 °C for 1 h. After hydration the dispersion was homogenized in M-110EH Microfluidizer® Processor (Microfluidics, USA) at 1500 bar. The resulting vesicles was ~60 nm in diameter. The zeta average size of vesicles was analyzed using quasi-elastic light scattering (Zetasizer Nano ZS; Malvern Instruments, UK). Before analysis, the samples were diluted in 0.9% NaCl with a volume ratio of 1/200. A total of four formulations were prepared, which were named LM-s, LM-p, LM-m and LM-m-L, respectively. The main differences among these formulations were different PC composition and PEG polymer grafting density (see Table 1 for more information)

2.3. Remote loading of liposomes

All the formulations were loaded using the same procedure. Briefly, a transmembrane ammonium sulfate gradient was generated across the vesicles by exchanging the extraliposomal buffer using Sephadex G-75 columns. The buffer employed in the experiments was sucrose (300 mM)–histidine (10 mM) buffer (pH 7.5). MIT was mixed with empty liposomes exhibiting a transmembrane gradient in a MIT/lipid mass ratio of 1/16, and then the mixture was incubated at 60 °C for 40 min. After loading, samples of the mixtures were taken and unentrapped MIT was removed by size exclusion chromatograph for determining the loading efficiency.

2.4. In vitro release studies

Drug release experiments were performed in three different release buffers. The liposomes were firstly diluted using the release media, to a PC concentration of 0.46 μmol/mL; and then 2 mL diluted liposomes were put into dialysis tubing with a molecular weight cutoff of 10,000, and dialyzed against 50 mL (for medium ii or iii) or 400 mL (for medium i) release buffers at 37 °C. Release buffer i isotonic glucose/histidine/NH_4Cl buffer (250/10/40 mmol/L) with a pH 7.5; release buffer ii 50% human plasma: 50% isotonic glucose/histidine buffer (290/10 mmol/L, pH 7.5); release buffer iii 50% human plasma plus 50% buffer i. Each buffer contained 100 μg/mL penicillin and streptomycin. The samples were withdrawn at specific time points and stored at −20 °C until analysis. The samples were treated and analyzed using method mentioned in PK studies.

Each experiment was repeated for at least twice, and the mean values were used to calculate the release parameters. The exponential regression was performed using SPSS software (11.5 version).

2.5. Acute toxicity evaluation

For the purpose of comparing the toxicities of different MIT formulations, liposomal MIT formulations and f-M were administrated to male balb/c mice at a dose of 6 mg/kg ($n = 10$). The reason of the employment of balb/c mice was that balb/c mice, a kind of inbred mice, were more sensitive to the toxicity induced by MIT. In the previous studies using a small amount of animals, it was proved that 6 mg/kg might be the maximum tolerance dose of free MIT. Because at the dose level, it was hard to discriminate the relative toxicity of LM-s, LM-p and LM-m-L, in the subsequent experiment, these three liposomal formulations were administrated at a dose level of 12 mg/kg. During the experimental period, qualified animal care technicians monitored the mice for weight loss and other signs of stress/toxicity for a period of 21 days. Because death cannot be used as an end point, mice were sacrificed at the first sign of distress for humane consideration. After 21 days, all remaining animals were terminated, and necropsies were conducted to identify any additional drug toxicities. The difference in body weights was examined by a series of independent-samples *T*-test and $p < 0.05$ was considered to be statistically significant. In addition, the survival time was analyzed using SPSS software (11.5 version, survival analysis).

2.6. Pharmacokinetic and biodistribution studies

A total of three experiments were performed. (1) Plasma pharmacokinetic analyses of four liposomal MIT formulations and free MIT were performed in normal KM mice; (2) normal balb/c mice was employed to investigate the difference in biodistribution of LM-p, LM-m and LM-m-L; (3) KM mice bearing a s.c. S180 tumor (0.5–0.7 cm^3) was used in comparative tissue distribution studies of both LM-s and free MIT.

For PK studies, KM mice received injections of 4 mg/kg single i.v. bolus dose of liposomal MITs and free MIT via tail vein. Blood samples were obtained via cardiac puncture under anesthesia and collected in Eppendorf tubes containing sodium heparin as an anticoagulant. For biodistribution studies, all formulations were administrated at a dose of 4 mg/kg. At the indicated time points, mice were euthanized. Liver, spleen, kidney, lung, heart, intestine and tumor were rapidly excised, rinsed in ice-cold normal saline, and snap frozen. Blood samples were centrifuged at 2500 rpm for 10 min to separate the plasma. The plasma and tissue samples were stored at −20 °C until additional analysis.

MIT concentrations in plasma, and normal and tumor tissue samples were determined using HPLC method. Before analysis, mouse tissues were firstly homogenized using a tissue tearor equipped with a 7-mm probe (Biospec Products, Inc., USA). A 10% (w/v) homogenate was prepared in 20% ascorbic acid solutions. For 150 μL plasma or tissue homogenate, 150 μL extraction solution (methanol containing 0.5 M HCl:acetonitrile (90/10, v/v)) was added. The resulting mixture was vortexed and permitted to precipitate at −20 °C for at least 1 h; and then centrifuged at 20,000 × *g* for 10 min. The supernatant was collected for analysis. The injection volume for samples was 20 μL.

A Waters HPLC system controlled by Millennium 32 software was used for chromatographic analysis, which was composed of 2690 liquid chromatograph and 996-diode array detector. The HPLC separations were achieved using a Zorbax C18, 150 mm × 4 mm i.d., 5 μm particle size column. The isocratic mobile phase was a mixture 30 volumes of acetonitrile and 70 volumes of a solution containing 6.0 g/L of sodium 1-heptanesulfonate and 9.0 mL/L of glacial acetic acid, running at a flow rate of 1 ml/min. Detection was accomplished at 650 nm. The retention time for MIT was ∼10 min, the recovery of drug was >95% and the standard curve with an *r*-value of 0.999.

The pharmacokinetic variables, tissue AUC, C_{max} were calculated using DAS 2.0 software (the net for drug evaluation of China).

2.7. Antitumor efficacy

S-180 tumor cells were injected s.c. (5×10^5 cells/mouse) in the right flank region of KM mice. Tumors were allowed to grow to a mean tumor volume of 0.1–0.2 cm^3 before initiation of treatment. Tumor-bearing mice were randomly divided into five groups ($n = 8$). The treatment groups were given a single i.v. injection of LM-s and free MIT (4 and 6 mg MIT/kg), respectively. Control mice were treated with an isotonic sucrose–histidine solution. The tumor volume (V) was calculated according to the equation $(\pi/6) \times \text{width}^2 \times \text{length}$. Animal weight and tumor sizes were monitored every 2 (or 3) days. For statistical analysis, the tumor volumes of treatment group and control at each time point were examined using one-way analysis of variance. Post hoc comparison of the means of individual groups was performed using LSD test. In all cases, $p < 0.05$ was considered to be statistically significant.

Table 2
In vitro release studies of liposomal mitoxantrone formulations

Formulation	Release Media	*r* value	*p* value	*k*	Half life (h)
LM-s	I	0.913	0.000	0.0061	113.63
	II	0.898	0.015	0.0160	43.32
	III	0.958	0.000	0.0293	23.66
LM-p	I	0.898	0.000	0.0085	81.55
	II	0.930	0.007	0.0180	38.51
	III	0.951	0.000	0.0315	22.00
LM-m	I	0.986	0.000	0.0257	26.97
	II	0.904	0.013	0.0217	31.94
	III	0.951	0.000	0.0389	17.82
LM-m-L	I	0.993	0.000	0.0503	13.78
	II	0.973	0.005	0.0490	14.15
	III	0.954	0.003	0.0887	7.81

The liposomes were diluted using the release media, to a PC concentration of 0.46 μmol/mL; and then 2 mL diluted liposomes were put into dialysis tubing with a molecular weight cutoff of 10,000, and dialyzed against 50 mL (for medium ii or iii) or 400 mL (for medium i) release buffers at 37 °C. release buffer i isotonic glucose/histidine/NH_4Cl buffer (250/10/40 mmol/L) with a pH 7.5; release buffer ii 50% human plasma: 50% isotonic glucose/histidine buffer (290/10 mmol/L, pH 7.5); release buffer iii 50% human plasma plus 50% buffer i. The samples were withdrawn at specific time points and analyzed using HPLC method described in Section 2. Each experiment was repeated for at least twice, and the mean values were used to calculate the release parameters. The regression was performed using SPSS software (11.5 version) and the data were fitted into exponential equation was $y = y_0 \times e^{-kt}$, where y_0 is initial encapsulation efficiency (%), y is %EE at time t, and k is for release constant. Half-life was determined by LN (2)/k.

3. Results

3.1. Preparation of liposomal MIT formulations

All the liposome-encapsulated MITs were prepared using ammonium sulfate gradient method. The formulation information is presented in Table 1. The main distinction among these formulations was that the vesicles were made from different PCs. The PCs used to form lipid bilayer in LM-s, LM-p and LM-m formulations were HPSC, DPPC and DMPC, respectively. Relative to other formulations, LM-m-L had low PEG grafting density. Microfluidization was employed to reduce the size of vesicles after the formation of MUVs in 0.3 M ammonium sulfate solutions, and all the resulting vesicles had uniform size distribution. At a drug to lipid molar ratio of 0.2, all the formulations exhibited a trapping efficiency approaching 100%.

3.2. Drug release rate

MIT was loaded into SUVs in response to a transmembrane ammonium sulfate gradient, thus free ammonium could deplete transmembrane gradient, resulting in the release of MIT. Drug release experiment was firstly performed in 40 mM NH_4Cl-containing medium using a dialysis method. Under these conditions, the release should be attributed to “dilution effect” and the triggering of ammonium. As shown in Table 2, the calculated release half-lives increased with increased T_m of PC, consistent with theoretical prediction. However, it is surprising to find that low pegylation formulation has a fast release rate (LM-m versus LM-m-L).

In 50% human plasma, the trend towards increased drug release kinetics as T_m of PC and PEG grafting density are decreased was also observed. It should be noted, though, that the driving force might be distinct from above case, since plasma ammonium concentration is extremely low and the liposomes were dialyzed against a small volume of plasma. Previous studies have proved that MIT has strong affinity to plasma proteins, thus the binding with proteins might drive the release of MIT from vesicles. For LM-m-L, a low pegylation

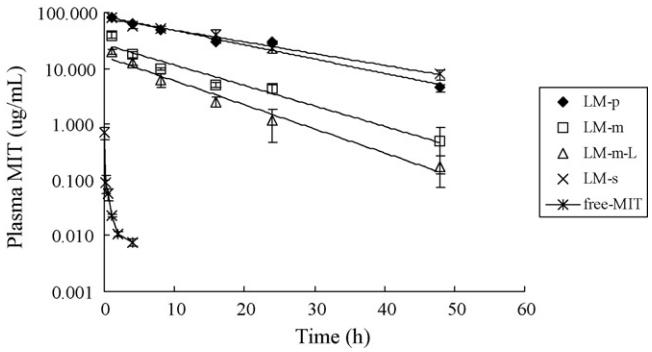

Fig. 1. Plasma concentrations of MIT in normal KM mice injected with liposomal MITs. Different liposomal MIT formulations and free MIT were injected into male KM mice (18–22 g, 6–8 weeks) via lateral tail veins at a dose level of 4 mg/kg (injection volume: 10 mL/kg). At specified time points, the mice were sacrificed and the blood was sampled via cardiac puncture. The total plasma MIT concentrations were determined using HPLC method described in Section 2. The data were shown as mean values ± S.D. ($n = 3$). To reveal the exponential clearance of liposomal MITs, the regression lines were added in the figure.

formulation, it still had the fastest release rate. It is possible that some kinds of proteins, especially lipoproteins could approach its surface due to incomplete PEG polymer coverage and affect the integration of lipid membrane.

When drug release studies were performed in NH_4Cl-containing plasma, the release kinetics was considerably accelerated for all the cases, indicative of the synergistic effect of ammonium and plasma.

3.3. Plasma pharmacokinetics

Following intravenous injection into mice at a dose of 4 mg/kg, the four liposomal formulations exhibited distinct plasma concentration versus time profiles (Fig. 1). Both LM-s and LM-p were slow release formulation, with the V_d values of ~0.9 mL, approximately equal to the plasma volume of a 20-g mouse. However, for formulations made from fluid PC, the V_d values were significantly larger than the volume of central compartment, suggestive of marked drug release from vesicles in circulation, and subsequent rapid distribution into local tissues. Free MIT had the largest V_d, analogous to previously reported result. By comparing the PK parameters of liposomal formulations with those of free MIT, it is easy to find that the encapsulation within vesicles could enhance the retention of MIT in plasma to varying degree. Interesting, the results from PK studies were well correlated with in vitro release data. Briefly, fast release formulation had increased V_d, clearance rate and K_e values, and decreased $T_{1/2}$ and AUC values (Table 3).

Table 3
Pharmacokinetic parameters of different MIT formulations in KM mice

Parameter	LM-s	LM-p	LM-m	LM-m-L	FM
$T_{1/2}$ (h)	14.43	11.59	8.60	6.96	0.98
AUC $_{0-48}$ (mg/(L h))	1538.3	1432.0	320.6	173.2	0.278
$AUC_{0-\infty}$ (mg/(L h))	1792.3	1595.6	368.5	196.3	0.404
K_e (1/h)	0.048	0.060	0.081	0.100	0.710
V_d (mL)	0.883	0.838	2.694	4.090	558.1
Cl (mL/h)	0.042	0.050	0.217	0.408	396.5

Different liposomal MIT formulations and free MIT were injected into male KM mice (18–22 g, 6–8 weeks) via lateral tail veins at a dose level of 4 mg/kg (injection volume: 10 mL/kg). At specified time points, the mice were sacrificed and the blood was sampled via cardiac puncture. The total plasma MIT concentrations were determined using HPLC method described in Section 2. The mean plasma MIT concentration values were used to calculate the pharmacokinetic parameters. To determine the parameters, DAS2.0 software was employed.

3.4. Acute toxicity

To compare the relative toxicity of different formulations, MIT formulations were injected into balb/c mice at a dose of 6 mg/kg, a dose corresponding to the maximum tolerance dose of free MIT in previous studies. The animals treated with LM-m-L, LM-p and LM-s exhibited minor body weight loss, with maximum loss not exceeding 15% of original weight, and no significant difference among these three groups had been found. In f-M group, three mice had consistent weight loss of 20% for 72 h, and were sacrificed for human consideration. To our surprise, LM-m was more toxic than free MIT at this dose level. All the mice were sacrificed because of severe weight loss, resulting in a median survival time of 4.00 ± 0.79 days.

For the purpose of further evaluation of relative toxicity of LM-s, LM-p and LM-m-L, the animals were treated with MIT formulations at an elevated dose, 12 mg/kg, at which dose LM-s can be well tolerated by mice. Based on survival data, it was easy to find that the order of toxicity was LM-s < LM-p < LM-m-L < f-M < LM-m (Table 4). In addition, the toxicity induced by 12 mg/kg LM-s was equivalent to that induced by 6 mg/kg f-M, revealing that LM-s was at least two times less toxic than free MIT in balb/c mice.

3.5. Tissue distribution of LM-p, LM-m and LM-m-L

It was surprising to find that LM-m was more toxic than other formulations. To elucidate the phenomenon, the biodistribution studies were undertaken. As presented in Table 5, in heart and lung, the deposition of these formulations had almost no distinctions. However, the biodistribution of liposomal formulations in other organs exhibited marked difference. LM-m preferentially accumulated into kidney, resulting in the highest AUC values of 1037.6 μg/(g h). In contrast, LM-m-L, the formulation with low PEG coverage had a tendency to deposit in to RES rich organ such as liver and spleen, with a total AUC value in both organs of 825.4 μg/(g h). Because both formulations were fast release formulation, the large tissue AUC values might mean the considerable exposure of these main organs to bioavailable MIT (released MIT). Therefore, the increased toxicity of LM-m might be ascribed to kidney impairment induced by MIT.

Table 4
Acute toxicity studies

Treatment groups	Dose level (mg/kg)	Mean survival time (days)	Median survival time (days)	>21 days survivors
f-MIT	6	17.20 ± 1.84	n.a.	7/10
LM-m	6	4.50 ± 0.40	4.00 ± 0.79	0/10
LM-m-L	12	7.70 ± 0.21	8.00 ± 0.19	0/10
LM-p	12	10.90 ± 1.14	10.00 ± 0.36	1/10
LM-s	12	17.50 ± 1.72	n.a.	7/10

Acute toxicity study was performed in male balb/c mice with a body weight ranging from 18 to 20 g. Different MIT formulations were injected into mice via tail veins at a MIT dose of 6 or 12 mg/kg. Following administration, mice were monitored daily by qualified technicians. Provided that there was a rapid or consistent body weight loss >20% of original weight maintaining for 72 h, the mice were sacrificed for human considerations.

Table 5
Biodistribution of MIT in important organs following the injection of liposomal MITs

Tissues	AUC $_{0-48}$ (μg/(g h))			Range of tissue concentration (μg/g)		
	LM-p	LM-m	LM-m-L	LM-p	LM-m	LM-m-L
Heart	153.1	113.5	116.6	2.60–3.84	1.30–3.68	1.59–3.52
Liver	371.4	183.6	289.5	4.95–10.62	2.38–5.24	4.21–8.62
Spleen	489.0	277.8	591.3	6.84–11.63	5.08–7.33	10.54–18.21
Lung	267.3	257.2	234.1	2.79–7.71	3.45–6.89	4.47–5.75
Kidney	375.1	1037.6	522.6	6.43–9.95	11.66–28.99	7.45–14.34

Different liposomal MIT formulations were injected into male balb/c mice (18–22 g, 6–8 weeks) via lateral tail veins at a dose level of 4 mg/kg (injection volume: 10 mL/kg). At specified time points, the mice were sacrificed and the tissue samples were excised. The total MIT concentrations in different tissues were determined using HPLC method described in Section 2. The mean MIT concentration values were used to calculate AUC values. To determine the parameters, DAS2.0 software was employed.

3.6. Biodistribution of LM-s in s-180 bearing KM mice

Tissue level of MIT was determined in S-180 bearing mice. Compared to f-M, LM-s preferentially accumulated into tumor zones, instead of normal tissues (Table 6). Tumor AUC in LM-s treated animals was ~12 folds higher than in mice treated with the same dose of f-M. Peak MIT concentration in tumor was higher and occurred later than after f-M treatment (16 h versus 4 h).

Except in liver, the C_{max} in all normal tissues following injection of LM-s significantly decreased. The C_{max} in heart, a primary target organ for MIT-associated toxicity, was 26% lower in LM-s group than in f-M group. Because cardiotoxicity is related to C_{max} but not to AUC, this result might imply the reduced cardiotoxicity of LM-s. Furthermore, the assay in this study could not distinguish between liposome-entrapped (non-bioavailable) and free MIT (bioavailable), the increased AUC and C_{max} in liver following LM-s administration might not mean the increased liver toxicity of LM-s, taking into account the slow drug release rate of LM-s. Acute toxicity study also supported the low toxicity of LM-s. The evaluation using other parameters such as AUQ, T_e and r_d gave the same conclusions, namely, LM-s could alter the biodistribution of MIT, and selectively delivered MIT into tumor, indicative of enhanced EPR effect.

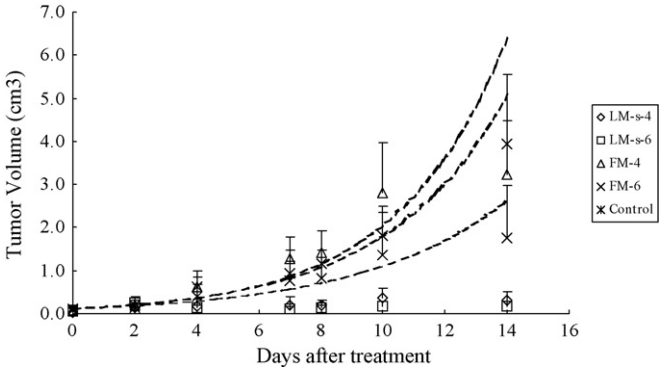

Fig. 2. Antineoplastic effects of LM-s and f-M formulations in S-180 solid tumor model. S-180 sarcoma cells (5×10^5 mouse^{-1}) were inoculated s.c. into the right frank regions of male KM mice. When the tumor volume reached 0.1–0.2 cm^3, LM-s and f-M were injected (i.v.) into mice via lateral tail veins at a dose level of 4 (or 6 mg/kg). Control group was treated with isotonic glucose/histidine buffer. Tumor width and length were measured with caliper and the volume was calculated in accordance with the formula of $v = \pi/6 \times \text{length} \times \text{width}^2$. The values were shown as mean ± S.D. ($n = 8$). For tumors with rapid growth rate, exponential trend lines were added. The regression equations were as follows: control: $v = 136.25 \exp(0.2584t)$, $r = 0.975$; f-M (4 mg/kg): $v = 119.94 \exp(0.2842t)$, $r = 0.93$; f-M (6 mg/kg): $v = 128.42 \exp(0.2156t)$, $r = 0.9647$.

3.7. Antitumor effects

The antineoplastic effects of LM-s and f-M were evaluated using s-180 solid tumor model (Fig. 2). 5×10^5 tumor cells were inoculated into KM mice, and when the mean tumor volume reached 0.1–0.2 cm^3 (6–8 mm in diameter), the treatment was initiated. During the experimental period, the tumors in control group rapidly grew, with a mean doubling time of 2.68 days. The administration of free MIT at different dose (4 or 6 mg/kg) had almost no therapeutic effects, compared with control group. The mean tumor doubling time for 6 and 4 mg/kg free MIT group was 3.21 and 2.44 days, respectively. On the contrary, LM-s exhibited considerable antitumor efficacy; and the growth of s-180 tumor was markedly inhibited. Fourteen days post-treatment, the tumor volume inhibition in 4 and 6 mg/kg LM-s group was 92.35 and 95.79%, respectively. As indicated by these data, the encapsulation of MIT into pegylated HSPC/chol vesicles could significantly improve the antineoplastic effect. Furthermore, the

Table 6
Percentage of MIT distributed to various tissues of s-180 bearing KM mice

Tissues	LM-s				Free-MIT				r_d
	$AUC_{0-24\,h}$ (μg h/g)	C_{max} (μg/g)	$AUQ_{0-24\,h}$ (μg h)	T_e	$AUC_{0-24\,h}$ (μg h/g)	C_{max} (μg/g)	$AUQ_{0-24\,h}$ (μg h)	T_e	
Heart	71.65	4.01	8.73	1.32	78.59	5.39	9.08	2.21	0.60
Liver	140.23	6.78	264.21	40.04	64.07	4.77	115.05	27.95	1.43
Spleen	137.38	7.56	23.63	3.58	123.45	7.75	17.09	4.15	0.86
Lung	123.41	8.44	21.06	3.19	183.33	10.21	30.87	7.50	0.43
Kidney	158.62	7.12	66.07	10.01	290.45	18.24	119.35	28.99	0.35
Intestine	53.88	2.42	91.37	13.85	67.55	3.94	109.17	26.52	0.52
Tumor	248.52	14.75	184.78	28.00	20.06	1.26	11.07	2.69	10.41
Total			659.85	100.00			411.69	100.00	

S-180 sarcoma cells (5×10^5 mouse^{-1}) were inoculated into s.c. the right frank regions of male KM mice. When the tumor volume reached 0.5–0.7 cm^3, LM-s and f-M were injected (i.v.) into mice via lateral tail veins at a dose level of 4 mg/kg. At specified time points, the mice were sacrificed and the tissue samples were excised. The total MIT concentrations in different tissues were determined using HPLC method described in Section 2. The mean MIT concentration values were used to calculate AUC values. To determine the parameters, DAS2.0 software was employed. The weighted-average overall drug targeting efficiency (T_e) was calculated according to the equation: $T_e = AUQ_i / \Sigma(AUQ)_j \times 100$. Where i refers to the target tissue, and j refers to each tissue. AUQ refers to the area under MIT amount-time curve, which can be obtained by multiplying AUC and tissue weight of each tissue. The r_d value equals to $(\%\ \text{drug distributed})_{LM\text{-}s} / (\%\ \text{drug distributed})_{f\text{-}M}$.

relative toxicity of different MIT formulations could be also roughly evaluated using body weight loss data. The order of maximum body weight loss usually occurred at 7 days after treatment, and the order of it was LM-s-4 mg/kg (8.5%) < LM-s-6 mg/kg (11.5%) < f-MIT-4 mg/kg (17.5%) < f-MIT-6 mg/kg (20.5%). Accordingly, LM-s formulations could reduce the toxicity of free MIT in KM mice, too.

4. Discussion

In this study, MIT was encapsulated into pegylated SUVs, with transmembrane ammonium sulfate gradient. A total of four formulations were prepared, which were made from different PCs, and had distinct PEG grafting density. The drug release rates from these vesicles are different, and could be ordered as follows: LM-s < LM-p < LM-m < LM-m-L. However, the release mechanism in different buffers might be different. In NH_4Cl buffer, the main driving forces that promote drug release are the dilution effect and the depletion of pH gradient. In human plasma, the presence of plasma protein should be regarded as impetus. Based on drug release experiments, it is found that the drug release rate increases with decreased T_m of PCs, and reduced grafting density of PEG polymer. It is easy to understand the effect of T_m of PCs on drug release rate, because the lipid membrane made from fluid PCs will be in lipid crystalline status at body temperature, thus permitting the rapid drug release (Drummond et al., 1999). But why the vesicles with low PEG coverage has fast drug release rate? To resolve this question, the conformation of PEG polymers on the vesicles should be taken into account. The conformation of PEG depends on the PEG grafting density and peg molecular weight, which could be divided into three regions, namely, interdigitated mushroom, mushrooms and brush conformations (Kenworthy et al., 1995; Needham and Dewhirst, 2001; Mills and Needham, 2004). In our study, PEG_{2000}-DSPE is employed, and except LM-m-L formulation, other formulations have a PEG molar percent of ~8%. Therefore, on the surface of LM-m-L vesicles, the PEG polymer should be arranged as interdigitated mushrooms, compared to the brush conformation on the surface of other vesicles (Kenworthy et al., 1995). The incomplete PEG coverage on vesicle surface might permit the adhesion of plasma lipoprotein to vesicles in human plasma, thus facilitating MIT release. However, in release buffer without plasma, low pegylation formulation still has fast release rate. Therefore, we suspect that the high pegylation degree might preclude the MIT release because MIT (a multivalent ammonium) could interact with PEG-lipid (a negative polymer) via electrostatic effects.

In plasma, fast release formulation had decreased $T_{1/2}$, too. The plasma kinetics of MIT is determined by the clearance kinetics of vesicles from plasma, and the drug release rate from vesicles. For LM-s, LM-p and LM-m, the clearance kinetics of vesicles might be same, and the drug release rate might be the single determinant factor since all of them have complete pegylation. However, in the case of LM-m-L, the low PEG grafting density makes it hard to evade the recognition by RES system, and endocytosis might accelerate its clearance.

The exposure of important healthy organs to free MIT is responsible for the toxicity of different formulations. However, it is difficult to distinguish liposome-encapsulated MIT from free MIT in tissues simultaneously. We could only roughly correlated tissue AUC values with the toxicity data. Provided that fast release formulations considerably deposit in a specific organ, and lead to a large tissue AUC, it could be deduced that the formulation might be harmful to the organ. Based on these, it is concluded that LM-m is toxic to kidney, thus leading to the early death in acute toxicity studies.

Because the reduced toxicity of LM-s relative to other formulations, it was chosen for further studies. It is found that this formulation could effectively deliver MIT into tumor zones, resulting in ~12-fold increase in tumor AUC. Simultaneously, the distribution of LM-s into healthy tissue significantly decreased. The improved biodistribution leads to enhanced antitumor efficacy, too. In s-180 tumor model, treatment with LM-s results in >90% tumor inhibition ratio. However, at the same dose level, free MIT exhibits almost no therapeutic effects.

Our studies clearly reveal the influences of lipid composition and PEG polymer coverage on the biological activity of liposomal MIT formulations. The PEG polymer grafting density could affect the surface characteristics of vesicles, thus influencing the biodistribution of vesicles. In contrast, the kinds of PCs could determine the permeability of lipid bilayer, and then affect drug release rate from vesicles. The interaction of these two factors might determine the amount of drug delivered to local tissues, and the exposure of local tissues to bioavailable drugs, thus affecting the biological activity of liposomal MIT formulations. Therefore, it is important to discriminate the biological effects of formulation factors during the procedure of developing liposomal drugs. Based on our data, encapsulation of MIT into HSPC/chol SUVs with high pegylation might be an optimum selection.

References

Adlakha-Hutcheon, G., Bally, M.B., Shew, C.R., Madden, T.D., 1999. Controlled destabilization of a liposomal drug delivery system enhances mitoxantrone antitumor activity. Nat. Biotechnol. 17, 775–779.

Ahmad, A., Wang, Y.F., Ahmad, I., 2005. Separation of liposome-entrapped mitoxantrone from nonliposomal mitoxantrone in plasma: pharmacokinetics in mice. Methods Enzymol. 391, 176–185.

Chang, C.W., Barber, L., Ouyang, C., Masin, D., Bally, M.B., Madden, T.D., 1997. Plasma clearance, biodistribution and therapeutic properties of mitoxantrone encapsulated in conventional and sterically stabilized liposomes after intravenous administration in BDF1 mice. Br. J. Cancer 75, 169–177.

Cohen, B.A., Mikol, D.D., 2004. Mitoxantrone treatment of multiple sclerosis: safety considerations. Neurology 63, S28–S32.

Cui, J., Li, C., Guo, W., Li, Y., Wang, C., Zhang, L., Zhang, L., Hao, Y., Wang, Y., 2007. Direct comparison of two pegylated liposomal doxorubicin formulations: is AUC predictive for toxicity and efficacy? J. Control. Release 118, 204–215.

Drummond, D.C., Meyer, O., Hong, K., Kirpotin, D.B., Papahadjopoulos, D., 1999. Optimizing liposomes for delivery of chemotherapeutic agents to solid tumors. Pharmacol. Rev. 51, 691–743.

Fox, E.J., 2006. Management of worsening multiple sclerosis with mitoxantrone: a review. Clin. Ther. 28, 461–474.

Genne, P., Olsson, N.O., Gutierrez, G., Duchamp, O., Chauffert, B., 1994. Liposomal mitoxantrone for the local treatment of peritoneal carcinomatosis induced by colon cancer cells in mice. Anticancer Drug Des. 9, 73–84.

Gokhale, P.C., Pei, J., Zhang, C., Ahmad, I., Rahman, A., Kasid, U., 2001. Improved safety, pharmacokinetics and therapeutic efficacy profiles of a novel liposomal formulation of mitoxantrone. Anticancer Res. 21, 3313–3321.

Johnson, J.L., Ahmad, A., Khan, S., Wang, Y.F., Abu-Qare, A.W., Ayoub, J.E., Zhang, A., Ahmad, I., 2004. Improved liquid chromatographic method for mitoxantrone quantification in mouse plasma and tissues to study the pharmacokinetics of a liposome entrapped mitoxantrone formulation. J. Chromatogr. B Anal. Technol. Biomed. Life Sci. 799, 149–155.

Kenworthy, A.K., Hristova, K., Needham, D., McIntosh, T.J., 1995. Range and magnitude of the steric pressure between bilayers containing phospholipids with covalently attached poly(ethylene glycol). Biophys. J. 68, 1921–1936.

Koeller, J., Eble, M., 1988. Mitoxantrone: a novel anthracycline derivative. Clin. Pharm. 7, 574–581.

Lim, H.J., Masin, D., Madden, T.D., Bally, M.B., 1997. Influence of drug release characteristics on the therapeutic activity of liposomal mitoxantrone. J. Pharmacol. Exp. Ther. 281, 566–573.

Lim, H.J., Masin, D., McIntosh, N.L., Madden, T.D., Bally, M.B., 2000a. Role of drug release and liposome-mediated drug delivery in governing the therapeutic activity of liposomal mitoxantrone used to treat human A431 and LS180 solid tumors. J. Pharmacol. Exp. Ther. 292, 337–345.

Lim, H.J., Parr, M.J., Masin, D., McIntosh, N.L., Madden, T.D., Zhang, G., Johnstone, S., Bally, M.B., 2000b. Kupffer cells do not play a role in governing the efficacy of liposomal mitoxantrone used to treat a tumor model designed to assess drug delivery to liver. Clin. Cancer Res. 6, 4449–4460.

Madden, T.D., Harrigan, P.R., Tai, L.C., Bally, M.B., Mayer, L.D., Redelmeier, T.E., Loughrey, H.C., Tilcock, C.P., Reinish, L.W., Cullis, P.R., 1990. The accumulation of drugs within large unilamellar vesicles exhibiting a proton gradient: a survey. Chem. Phys. Lipids 53, 37–46.

Martinelli Boneschi F, Rovaris M, Capra R, Comi G. Mitoxantrone for multiple sclerosis. Cochrane Database of Systematic Reviews 2005, Issue 4. Art. No.: CD002127.
Mike, S., Harrison, C., Coles, B., Staffurth, J., Wilt, T.J., Mason, M.D., 2006. Chemotherapy for hormone-refractory prostate cancer. Cochrane Database Syst. Rev., CD005247.
Mills, J.K., Needham, D., 2004. The materials engineering of temperature-sensitive liposomes. Methods Enzymol. 387, 82–113.
Murray, T.J., 2006. The cardiac effects of mitoxantrone: do the benefits in multiple sclerosis outweigh the risks? Expert Opin. Drug Saf. 5, 265–274.
Needham, D., Dewhirst, M.W., 2001. The development and testing of a new temperature-sensitive drug delivery system for the treatment of solid tumors. Adv. Drug Deliv. Rev. 53, 285–305.
Neuhaus, O., Kieseier, B.C., Hartung, H.P., 2006. Therapeutic role of mitoxantrone in multiple sclerosis. Pharmacol. Ther. 109, 198–209.
Pestalozzi, B., Schwendener, R., Sauter, C., 1992. Phase I/II study of liposome-complexed mitoxantrone in patients with advanced breast cancer. Ann. Oncol. 3, 445–449.
Pestalozzi, B.C., Vass, A., Adam, H., Horber, D.H., Schwendener, R.A., Sauter, C., 1995. Phase II study of liposome-complexed mitoxantrone in patients with advanced breast cancer. Eur. J. Cancer 31A, 1024.
Samad, A., Sultana, Y., Aqil, M., 2007. Liposomal drug delivery systems: an update review. Curr. Drug Deliv. 4, 297–305.
Schwendener, R.A., Fiebig, H.H., Berger, M.R., Berger, D.P., 1991. Evaluation of incorporation characteristics of mitoxantrone into unilamellar liposomes and analysis of their pharmacokinetic properties, acute toxicity, and antitumor efficacy. Cancer Chemother. Pharmacol. 27, 429–439.
Tallman, M.S., Gilliland, D.G., Rowe, J.M., 2005. Drug therapy for acute myeloid leukaemia. Blood 106, 1154–1163.
Ugwu, S., Zhang, A., Parmar, M., Miller, B., Sardone, T., Peikov, V., Ahmad, I., 2005. Preparation, characterization, and stability of liposome-based formulations of mitoxantrone. Drug Dev. Ind. Pharm. 31, 223–229.
Wiseman, L.R., Spencer, C.M., 1997. Mitoxantrone. A review of its pharmacology and clinical efficacy in the management of hormone-resistant advanced prostate cancer. Drugs Aging 10, 473–485.